

Procedural aspects of modeling the dynamics of a three wheeled vehicle using ADAMS-CAR

Venkata Mangaraju Karanam¹, Anindya Chatterjee², Ashitava Ghosal³

¹ Research and Development, TVS Motor Company Ltd., Hosur, India.
venkata.raju@tvsmotor.co.in

² Mechanical Engineering, Indian Institute of Technology, Kharagpur, India.
anindya100@gmail.com

³ Mechanical Engineering, Indian Institute of Science, Bangalore, India.
asitava@mecheng.iisc.ernet.in

Original version: Aug 3, 2011

Version 3: Sep27, 2012

This document may be downloaded from <http://eprints.iisc.ernet.in/40423/>

Abstract

We describe in some detail the process of development of a dynamic model of a three wheeled vehicle using ADAMS-CAR. We first describe the rigid body model, and then the modeling of structural flexibilities. The aim of this report is to document procedural details of such modeling, with a view to presenting more research and development oriented investigations in the future. The contents of this report may also be of interest to practicing engineers engaged in multi-body dynamics modeling of wheeled vehicles.

1. Introduction:

This report presents a detailed description of dynamic modelling of a three wheeled vehicle using ADAMS-CAR. Such vehicles are commonly used in south Asian countries including India, but dynamic models for them have not been discussed in the engineering literature.

The automotive vehicle industry routinely uses multi-body dynamics (MBD) simulation software, like AUTOSIM, ADAMS, and DATZ, in its R&D work. A small representative sample of such work may be found in references [1-7], which deal with either two- or four-wheeled vehicles. There is also published work on *roll-enabled* three wheeled vehicles [8, 9]. However, in the three wheeled passenger vehicle shown in figure 1a, which we are concerned with here, roll angles are always small during normal operation. These vehicles are small and light, run at low speeds, have small wheels, and may qualitatively be viewed as four wheeled cars where the two front wheels have been replaced by a single one in the middle. In the roll-enabled three wheeled vehicles mentioned above, extra degrees of freedom allow large roll angles even while the two rear wheels maintain contact with the road. In our vehicle, there is no such degree of freedom.

In our on-going work, we are studying the dynamics and stability of these latter (low-roll) three wheeled vehicles. The aim of this report is to document, in some detail, the process of development of a dynamic model of such a vehicle using ADAMS-CAR. In our opinion, an engineer knowing the issues and methods discussed below can develop a model such as presented below in perhaps 12 to 15 weeks. The aim of this report is to provide a guide to such an engineer, as well as to place on record

the way in which we have developed this simulation with a view to more detailed, research oriented, simulation studies in the future.

This report resembles our earlier report [5] on motorcycle modelling, the main differences being (i) the use of ADAMS-CAR as opposed to ADAMS-Motorcycle and (ii) the incorporation of flexibility in the system.

Schematic diagrams of a three wheeler are shown in figures 1b and 1c. We begin with a rigid body model, with up to 52 degrees of freedom as follows:

- **6** degrees of freedom for the frame plus rigidly attached rider and passengers
- 3 rotations and 3 translations for each of two trailing arms (total: **12**) and 6 degrees of freedom for each rear suspension (total: **12**)
- **1** rotation at the steering pivot
- **3** wheel rotations
- 3 rotations and 3 translations of the front suspension, including small flexibilities of bushes (total: **6**) and **6** degrees of freedom of the trailing link.
- 3 rotations and 3 translations of the engine system (total: **6**)



Figure 1a: Picture of a three- wheeled passenger vehicle.

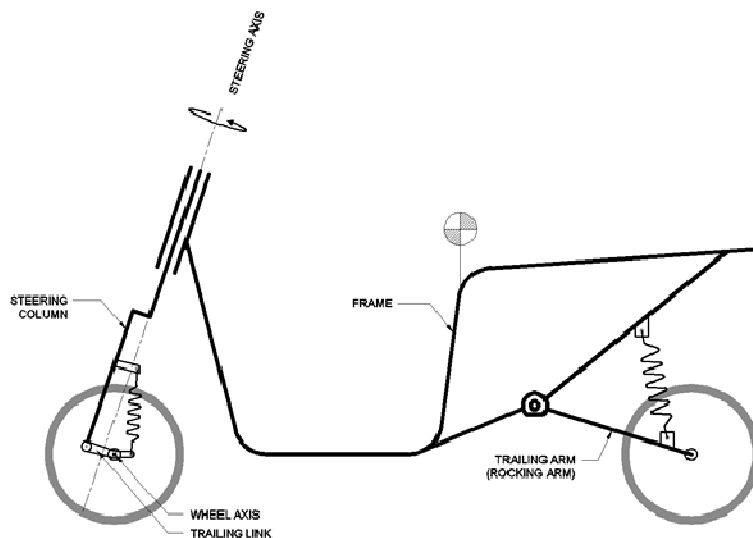


Figure 1b: A schematic of a three wheeled passenger vehicle.

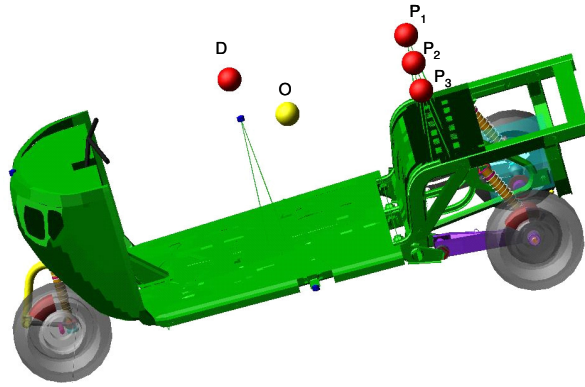


Figure 1c: Multi-body dynamic model of a three wheeler. In this figure D , P_1 , P_2 , P_3 and O represent the CG locations of the driver, three passengers and chassis.

Among the above degrees of freedom, two out of three rotations in each trailing arm occur due to rubber bush, and are small; the main rotation is mainly due to rear suspension displacement. The translational degree of freedom for the trailing arm is removed using a bush and spherical joint to attach it to the frame. The rear suspension is attached to the trailing arm and frame thru rubber bushes and joints in a way that the relative rotation between the frame, suspension and trailing arm depends on rubber bush torsional stiffness. This results in one degree of freedom for each rear suspension. Similarly, the front suspension is here restricted to have just one degree of freedom. With these simplifications, in this report we will consider a rigid body model with 25 degrees of freedom. These are: 6 degree of freedom for the frame plus rigidly attached rider, 6 degree of freedom for the powertrain, 3 rotations of each trailing arm (total 6), 1 rotation each rear suspension (total 2), 1 rotation at the steering pivot, 1 front trailing link rotation and 3 wheel rotations.

The dimensions and inertia properties of various components, as well as tire and suspension properties, can be incorporated into the ADAMS model and these are described below. Front and rear suspensions are modelled using spring and (nonlinear) dashpot elements.

The tire is geometrically modelled as a torus and tire-ground interaction is modelled using local stiffness and slip relations (using the famous Magic formula [11]). The tire modelling here differs from that used for two-wheeled vehicles in our earlier work [1, 5]. Here, we have used the simpler Pacejka-94 [12] tire model. The effects of relaxation length, camber and variation of load on tire characteristics are neglected in this model, and the number of coefficients used for each tire characteristic is smaller compared to other models like the Pacejka-2002 [13] tire model. For example, the number of coefficients included for the lateral stiffness characteristic curve is 17, compared to 34 in other recent models (see [11] for more details). While we have used a simplified Magic formula model for the tires, it is of course possible to use more complex models within ADAMS-CAR.

The model has four control or force/torque inputs. The first is a steer torque at the steering pivot (equal and opposite on the front fork assembly and the frame). The second is an engine forward drive torque, which acts through a drive train on the rear wheels (with reaction moment on the frame). The third and fourth inputs are front and rear wheel braking torques, applied in a user-specifiable ratio keeping the braking torque at the two rear wheels equal.

ADAMS allows road profiles [5], or paths, to be specified. It is also possible to specify the desired speed along the path. In such circumstances, there is an internal controller (essentially a black box using, as far as we know, some sort of PID and preview based control strategy) that determines

suitable control inputs so as to achieve the desired speed of motion along the desired path. The result of the simulation in ADAMS is animation of the motion, graphical (plotted) outputs, as well as numerical values of various state variables as functions of time.

We now present a detailed description of the dynamic model.

2. Detailed model description:

The model consists of eight different subsystems, which are defined and assembled together, to make the full vehicle assembly as shown in figure 1c. The subsystems are:

- Frame assembly
- Steering system assembly
- Front suspension assembly
- Trailing arm assembly (including shock absorbers)
- Brake system
- Power train
- Front wheel and rear wheels

Modeling a subsystem involves template creation, communicators, hard points, etc., more details of which are given in [5, 10].

2.1 Frame assembly:

The frame assembly includes several parts attached to the frame, such as the fuel tank, battery, seat, roof and various styling parts; but not the power train. A schematic is shown in figure 2. The frame assembly has the provision for attaching an engine system, steering system and two trailing arms. Additionally, four parts rigidly attached to it represent the driver and three passengers, each modelled as a point mass. The center of mass location and inertia properties of the frame assembly can be keyed in using a mouse-driven ADAMS window as shown in figure 2. Similarly individual properties can be given to the driver and three passengers. The topology, forces, parameter definitions, hard points and communicators are modelled as described in [5].

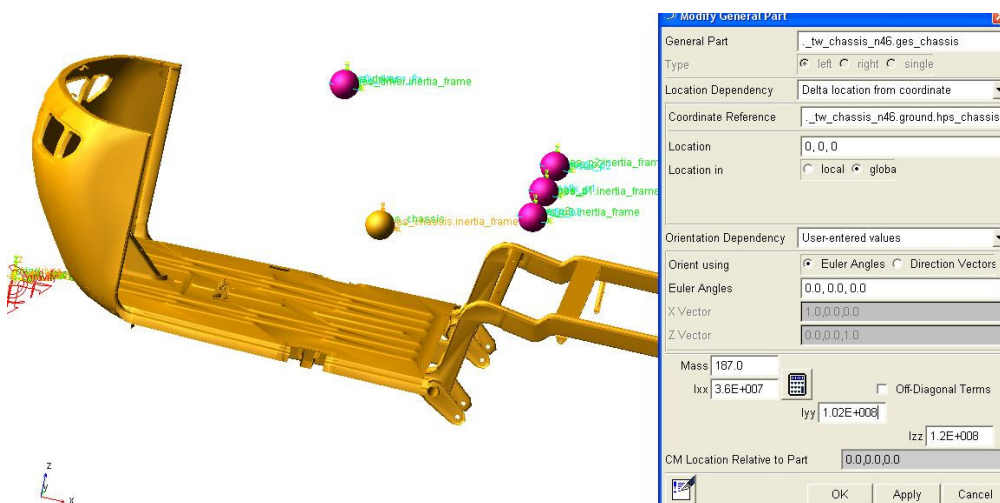


Figure 2: Schematic view of the frame assembly.

2.2 Steering system assembly:

All parts rotating together about the steering pivot, not including the front wheel, suspension and wheel-attached brake system parts, make up the steering system assembly (see figure 3a). This subsystem is attached to the frame through a revolute joint at the steering pivot. The front wheel is in turn connected to this subsystem through another subsystem called the front suspension. Center of mass location, inertia and suspension characteristics are input parameters.

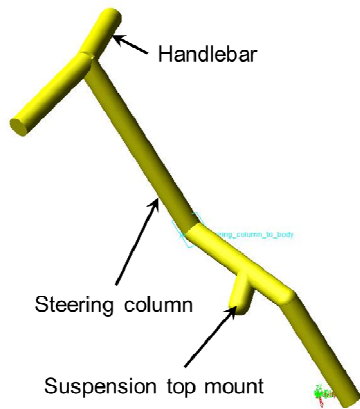


Figure 3a: Schematic view of steering system.

2.3 Front suspension:

The front suspension includes a spring and dashpot system, along with a Trailing link (also called “suspension lower mount”). See figure 3b. One end of the spring dashpot system is pivoted at an intermediate point on the steering column, and the other end of the spring dashpot system is pivoted at one end of the link. The other end of the link is in turn pivoted at the end of the steering column. In between these two end-pivots of the link is a third pivot point where the front wheel axle is mounted. The suspension pivots at top and bottom use a rubber bush (for properties, see appendix A) as shown in figure 3b. The spring stiffness used is around 25 N/mm and the damping is as shown in figure 3c.

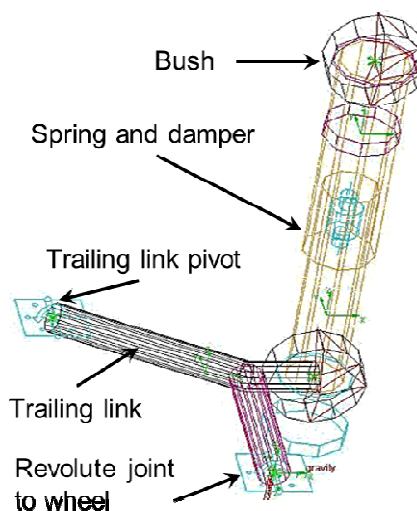


Figure 3b: Schematic view of front suspension system.

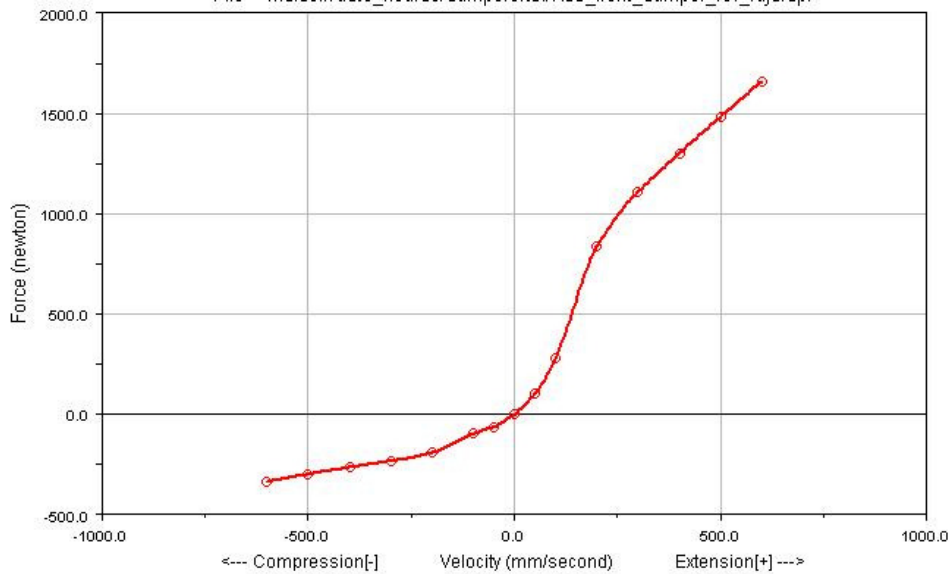


Figure 3c: Damping (dashpot force) curve of front suspension.

2.4 Rear suspension system:

The rear suspension system has two separate but symmetrical parts as shown in figure 4a (for the left and right sides of the vehicle). We describe one of them. There is a trailing arm, spring and dashpot system, rear wheel axle, and a drive shaft from power train to wheel. In the figure, the trailing arm pivot and the rear wheel axle are depicted as horizontal; and during normal motions they remain close to horizontal. The spring dashpot system is inclined as indicated. The drive shaft, though shown horizontal, is actually inclined in the assembled vehicle. The trailing arm is forked, and has two coaxially aligned rubber bushes through which it connects to the frame (for properties, see appendix B). One end of the spring dashpot system connects to the trailing arm through a rubber bush, and its other end connects to the frame through another rubber bush (similar to the front suspension: for properties, see appendix A). The spring stiffness is 48 N/mm and the damping (dashpot force) is as shown in figure 4b.

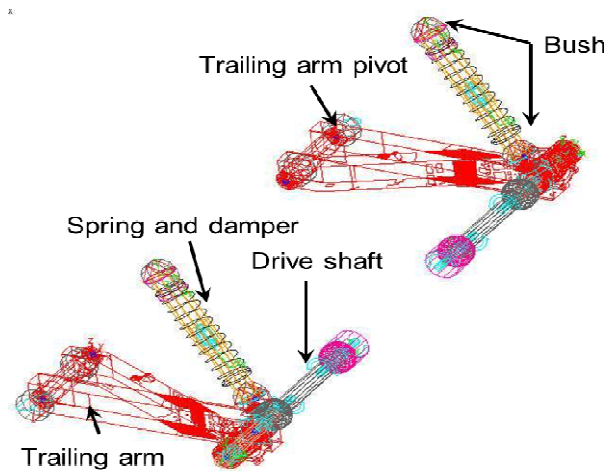


Figure 4a: Schematic view of Rear suspension system.

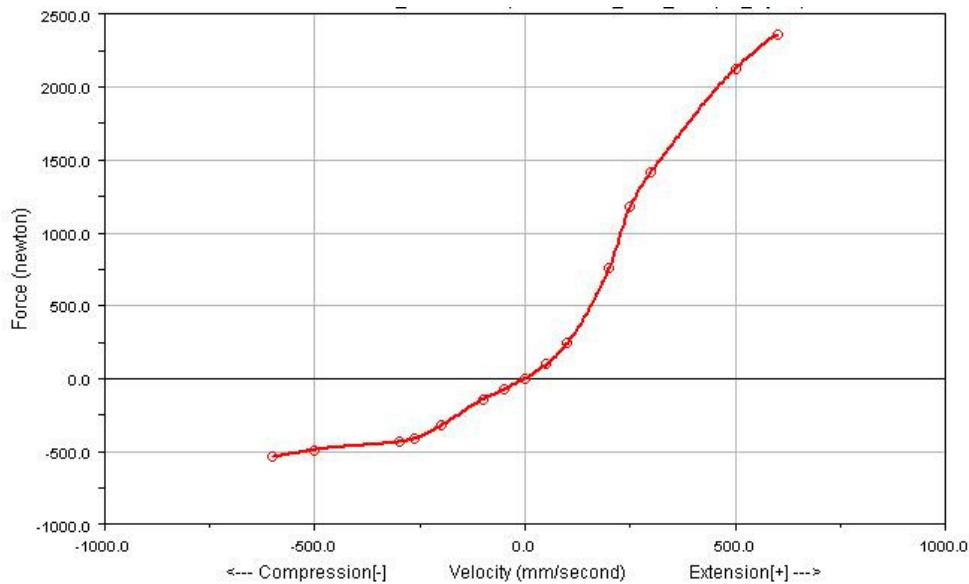


Figure 4b: Damping (dashpot force) curve for rear suspension.

2.5 Power train subsystem:

This represents the whole engine and includes the piston and cylinder assembly, exhaust system, crank shaft assembly and gearbox. A schematic view of the system is shown in figure 5. It has four bushes through which it is attached to the chassis. It has two revolute joints through which it connects to the shafts that in turn connect to the wheels. Idling RPM of the engine, clutch properties, engine torque, number of gears and gear ratios can be keyed in, or default values used: we used default values, because the goal of this simulation was to study vibration damping and stability characteristics on straight and curved paths, and not the effect of engine dynamics. CG location and inertia properties of the power train subsystem, of course, must also be keyed in, and for these we used parameters representative of a prototype.

2.6 Brake system:

Figure 6 shows a schematic view of the brake system. There is one disc for each rear wheel and one for the front. Inertias of these discs are included with corresponding wheels, so negligible values are assigned here.

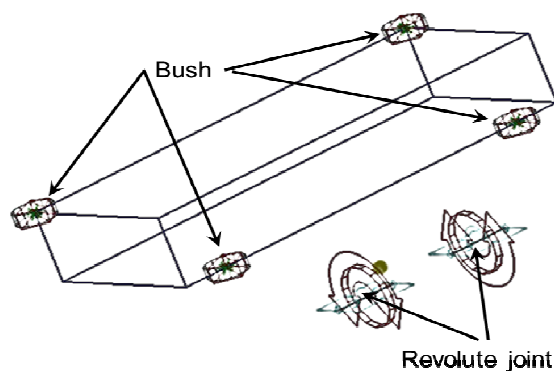


Figure 5: Schematic view of power train.

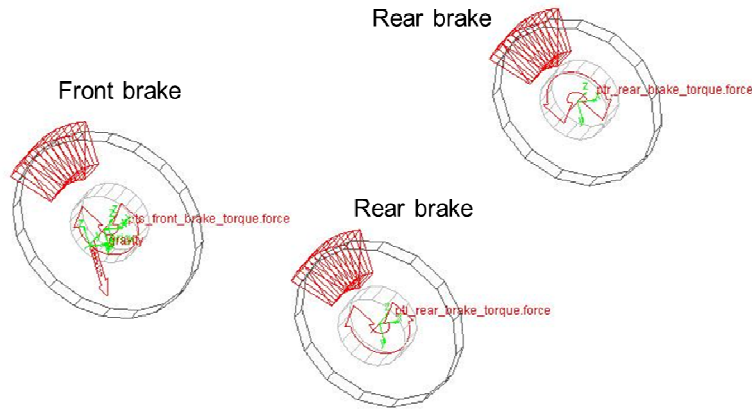


Figure 6: ADAMS's depiction of the brake subsystem.

2.7 Front wheel and rear wheels:

Figures 7a and 7b show schematic views of wheels, and a window that shows the properties to be keyed in. As shown in figure 7b, apart from mass and inertia properties, tire stiffness characteristics are input parameters for the wheel. An example of a tire property file is presented in appendix C.

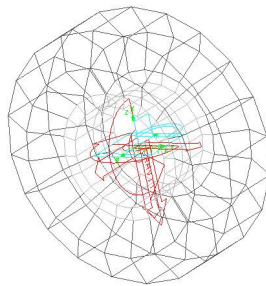


Figure 7a: Schematic view of front wheel.

2.8 Modeling of the front wheel:

So far our approach is largely similar to [5], except that the rear now has two forks and wheels. However, ADAMS-CAR is meant for four wheeled cars. Some issues relevant to three wheeled vehicles are as follows.

First, both front and rear suspensions of ADAMS-CAR use multiple links, but the suspension of our three wheeled vehicle is similar to that of the two wheeler of [5]. Further, the steering system of our three wheeled vehicle is similar to that of a two wheeled vehicle, and differs from cars. These two issues are addressed by defining new subassemblies as discussed above.

A remaining procedural issue is that the default model of ADAMS-CAR has two front wheels, and the three wheeled vehicle has only one. This issue is addressed through communicators, which were described in [5]. The default input communicators that supply wheel force information to the frame must be made to input zero forces, upon which the two default front wheels (not created in the model and not included in the subassembly) are eliminated. An additional front wheel subsystem is created

as above, and new communicators are defined for it, so that in the final assembly we have the desired three wheeled model. Put more simply, the two default front wheels are removed, and a new single front wheel is added.

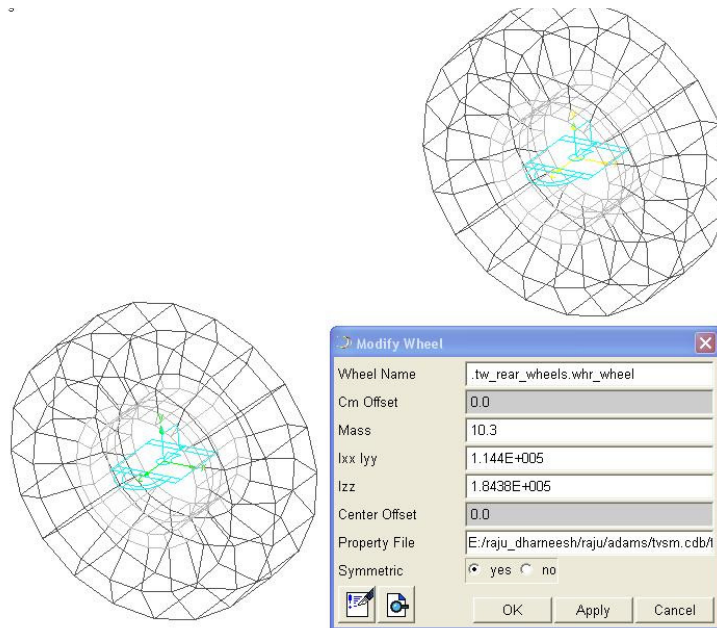


Figure 7b: Schematic view of rear wheels.

2.9 Vehicle parameters:

Using the eight subsystems described above, the three-wheeler model is assembled in ADAMS-CAR. Assembly requires that for the templates on each of the subsystems described above, appropriate input and output communicators were defined in advance (see [5] and the ADAMS manual for details).

Some model parameters are listed in tables 1 & 2. These values were used in the simulations reported here. The net wheel reaction forces for the stationary vehicle, and the net CG location, match our prototype vehicle within experimental measurement precision.

S.no	Vehicle parameter	Value
1	Wheel base	1980 mm
2	Wheel track	1150 mm
3	Trailing link length and angle	168 mm & 15 deg
4	Caster angle	19 deg
5	Steering offset	55 mm
6	Trailing arm length & angle	395 mm & 5.8 deg.
7	Front tire size (Radius × width)	203 mm × 101 mm
8	Rear wheel size (Radius × width)	203 mm × 101 mm

Table 1: Parameters of a typical three wheeled vehicle.

System	Mass	CG (m, m, m)	Inertia (Kg- m ²) [I _{xx} , I _{xy} , I _{yz} I _{yx} , I _{yy} , I _{xz} I _{zy} , I _{zx} , I _{zz}]
Steering system (without front tire)	6.385 kg	-0.0033, 0.031,0.454 From center of the front wheel. Part coordinate system is rotated by 19 deg. about 'Y' axis.	[1.85, 0.0223, 0.0312 0.0223, 1.83, -0.0110 0.0312, -0.0110, 0.1060]
Front wheel	10.3 kg	0, -0.0073, 0 From center of the front wheel.	[0.1140, 0.0, 0.0 0.0, 0.1840, 0.0 0.0, 0.0, 0.1140]
Frame assembly	488.27	1.376, 0, 0.629 From center of the front wheel.	[3460.0, 0.0382, 0.0268 0.0382, 3670.0, 385.0 0.0268, 385.0, 2430.0]
Front suspension	3.76	-0.006, 0.041, 0.0824 From center of the front wheel.	[0.0557, 0.0003, 0.00155 0.0003, 0.0335, 0.0062 0.00155, 0.0062, 0.0439]
Rear suspension	15.70	-0.0968, 0.575, 0.060 From the rear wheel center.	[9.150, -0.1030, -0.0543 -0.1030, 9.360, 0.0874 -0.0543, 0.0874, 1.020]
Power train	58	0.127, 0.575, 0 From the left side rear wheel center.	[19.50, 0.0, 0.0 0.0, 20.60, -4.123 0.0, -4.123, 11.5]
Rear wheel	10.3	Center of the wheel	[0.1140, 0.0, 0.0 0.0, 0.1840, 0.0 0.0, 0.0, 0.1140]

Table 2: Mass and inertia properties of a three wheeled vehicle. The moment of inertia matrices are defined using part coordinate systems (see also [5]). The part coordinate systems themselves are defined relative to the global XYZ axes. Where no rotation is specified, the part coordinate system in the vehicle reference configuration (or initial assembly) is taken to be perfectly aligned with the global XYZ axes.

3. Flexible MBD model:

The procedure described so far works for both rigid as well as flexible bodies. The representation of rigid bodies using geometrical shapes can be achieved within the ADAMS environment or imported from a drafting package like ProE or CATIA. However, general flexible bodies must be imported from compatible Finite Element Analysis (FEA) packages like ANSYS or NASTRAN using “.mnf” files. We have used ANSYS for .mnf file creation. The procedure is outlined here.

In the FEA mesh, nodes must be created at the locations where joints are desired (e.g., where joints were used in the erstwhile in rigid body model). These nodes have to be selected during .mnf file creation (see the ADAMS manual for details). Once the flexible body is imported into ADAMS, the remaining procedure of creating joints, communicators, hard points, etc., is the same as for the rigid body.

A simpler procedure may be used when we introduce flexibility effects into an already existing rigid body model. In the “template builder” session of ADAMS-CAR, the existing rigid body model of the relevant component is opened. Then, using the GUI, the .mnf file can be imported and the flexible component also appears on the screen. The joints, hard points, communicators etc. can now be transferred from the rigid body to the flexible body by choosing the “modify” option for these, which saves time compared to creating them again.

We mention that some simple flexible bodies (beam like) can be modelled directly within ADAMS, and offer the advantage of being easy to modify during parametric studies. However, we have used the above procedure due to the geometrical complexity of our components.

The ADAMS user guide [10] gives step by step instructions for the above operations and options.

The following three major structural components are modelled as flexible bodies within our three wheeled vehicle: (i) frame, (ii) steering column, and (iii) trailing arm. Descriptions follow.

3.1 Frame:

The frame consists of many parts joined with temporary as well as permanent joints. We modelled only the major structural parts that contribute to stiffness and strength, as shown in figure 8. In ANSYS, during .mnf file creation, several special nodes were created through which interfacing parts like the steering column, trailing arm, engine, etc., could be attached to the frame. We included 125 normal modes of the frame (the largest natural frequency is 1998.7 Hz). After creation of the .mnf file in ANSYS, the flexible body must be incorporated into the corresponding template. The GUI tab in figure 8 shows the input parameters and various options available for flexible bodies to be modified even within the full vehicle assembly. The tab modal ICs (for Initial Conditions) can be selected to specify modes to be retained in the dynamic analysis. Partial coupling and default damping options were chosen for the analysis (in partial coupling, ADAMS ignores some higher order terms in the inertia of flexible bodies; see [10]). Figure 9 shows some mode shapes of the frame (deformed as well as undeformed shapes).

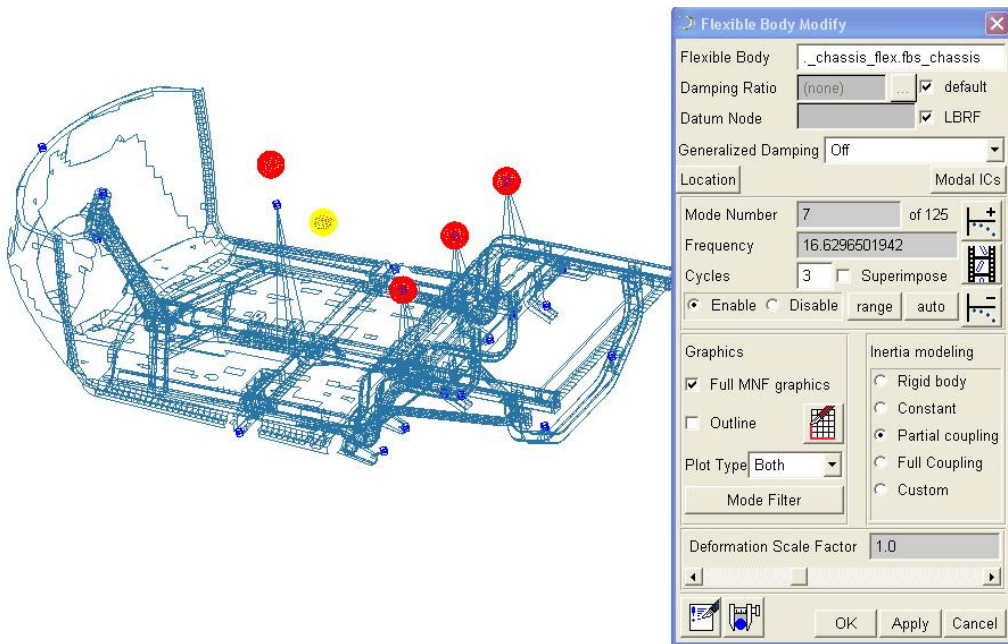
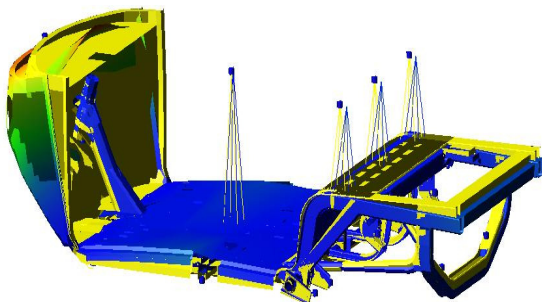
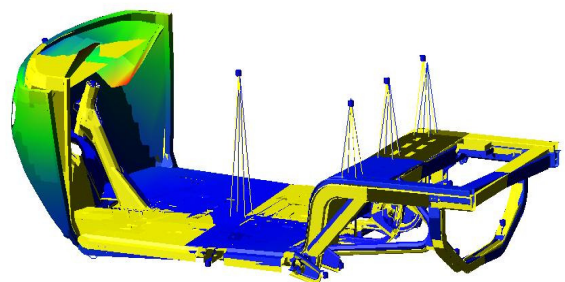


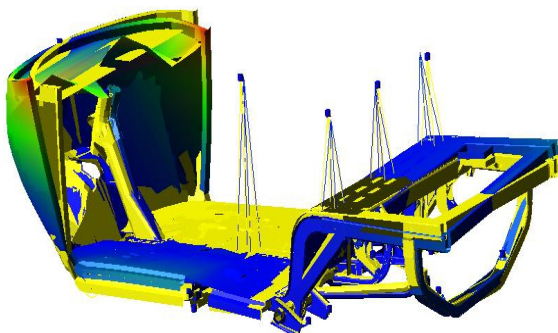
Figure 8: Flexible model of the frame.



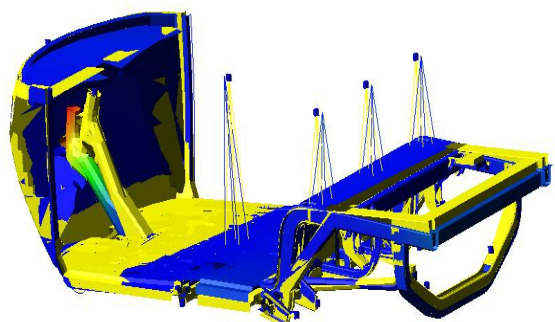
9th mode -15.93 Hz.



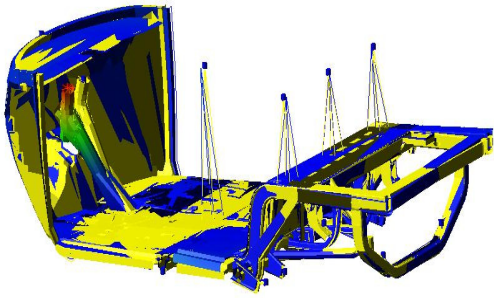
10th mode -16.17 Hz.



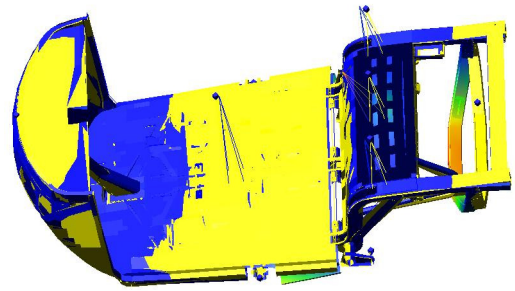
12th mode -29.84 Hz.



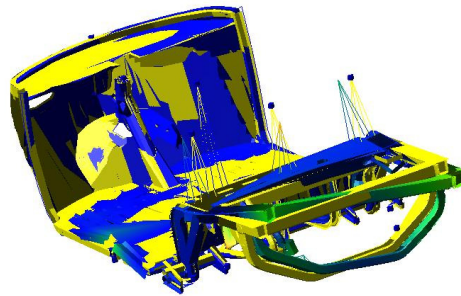
13th mode -30.82 Hz.



21st mode -60.60 Hz.



25th mode -83.37 Hz.



44th mode -144.15 Hz.

Figure 9: Different natural modes of frame.

3.2 Steering column:

In the steering column system only the column is treated as flexible. The handle bar is modelled as rigid (see figure 10), connected to the steering column at a node through a fixed joint. Similar to the frame, special nodes are created to attach frame, suspension and trailing link, and a few options are available to change some parameters at the assembly level. For this body we have retained up to the 13th mode (natural frequency 1653.2 Hz). Some mode shapes are shown in figure 11.

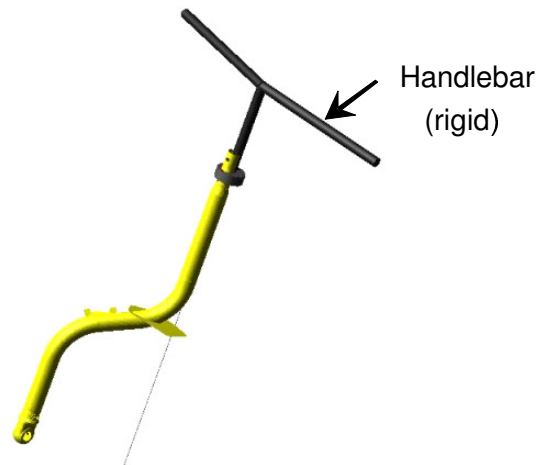


Figure 10: Flexible model of steering column.



7th mode -322.84 Hz.

8th mode -330.17 Hz.

Figure 11: Different natural modes of the steering column.

3.3 Trailing arm:

In the rear suspension system, the trailing arms are treated as flexible. Bodies connecting to the trailing arms (e.g., drive shafts; see figure 12) are modelled as rigid, connected to the trailing arms at nodes through fixed joints. Similar to the frame, special nodes are created to attach the frame, suspension and axle, and a few options are retained to change some parameters even after assembly. We retained 20 modes (highest frequency 1976.4 Hz). Some mode shapes are shown in figure 13.

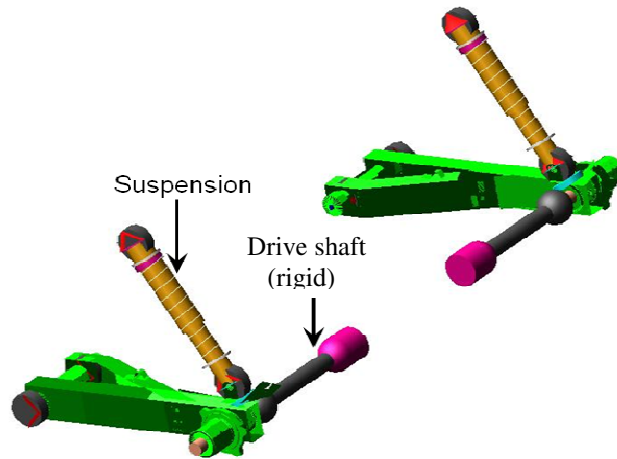
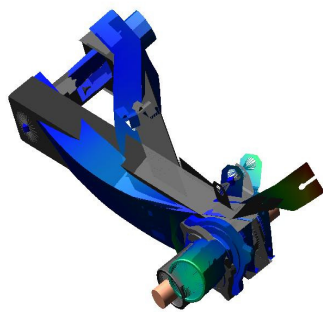
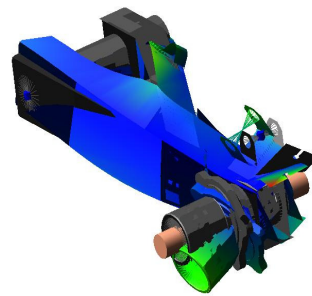


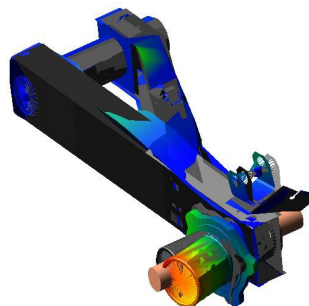
Figure 12: Schematic of rear suspension system with flexible model of trailing arm.



8th mode-819.23 Hz.



9th mode-885.67 Hz.



18th mode-1788.7 Hz.

Figure 13: Different natural modes of trailing arm (rocking arm).

4. Simulation procedure:

Using the eight subsystems described above, a three wheeled vehicle assembly can be created in ADAMS-CAR (similar to [5] for a motorcycle assembly). The model can then be used for various simulations [10].

In the ADAMS environment, once the model is ready on the screen, a choice of simulation can be chosen by selecting the ‘**simulate**’ tab as shown in figure 14. Subsequently, a dialog box allows input parameters to be entered before the simulation is run. Here, we have conducted three types of analyses as described below.

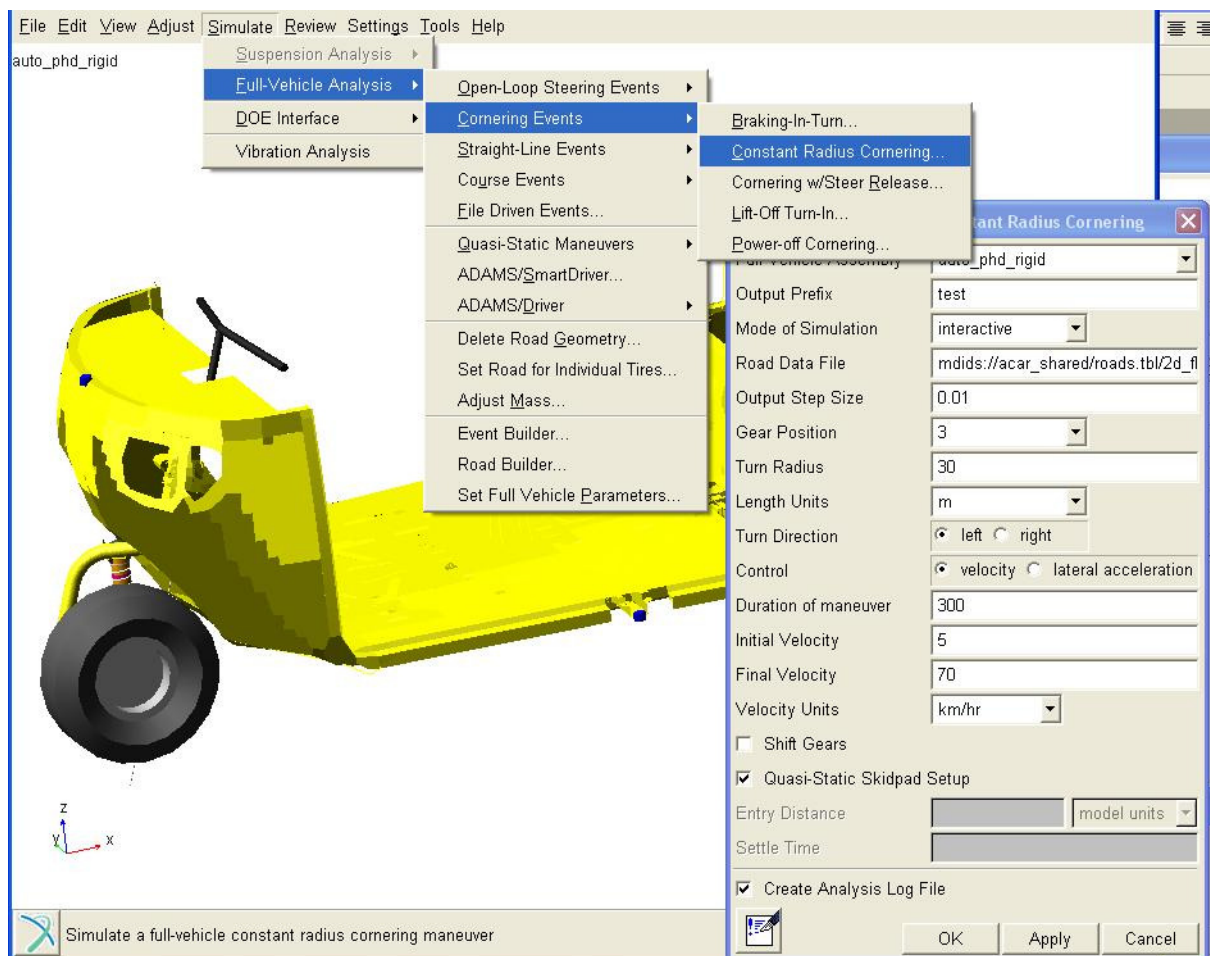


Figure 14: GUI of three wheeled vehicle and selection of simulation type.

4.1. Constant radius cornering:

In this section, we describe a constant radius cornering simulation (sometimes called a steering pad analysis). The relevant dialog box is shown in figure 14, in which the file name, simulation time, number of steps, path radius, direction of turn and lateral acceleration or speed range are the input parameters to be keyed in. We have run the simulation in *interactive mode*. Once the simulation is completed, results can be viewed using a post-processing window as shown in figure 15.

In the cornering simulation the vehicle first moves at a steady speed of 1.39 m/s (5 km/hr) along a straight path and is then accelerated along a circular path with acceleration of 0.06 m/s². A typical result of tire lateral slip is plotted in figure 15. Various other results could be plotted, like steering torque, steer angle and vehicle roll angle. In figure 15 the slip difference (difference between slip at the front tire and the average slip at the rear tires) is plotted against the speed of the vehicle. The slip is initially zero for both front and rear tires. Upon entering the circular path, there is a negative slip difference, i.e., the average rear tire slip exceeds the front tire slip. Near the end of the simulation the slip difference rises sharply and then falls to zero: this regime corresponds to loss of tire contact and rollover, as seen separately in animations as well (not included here).

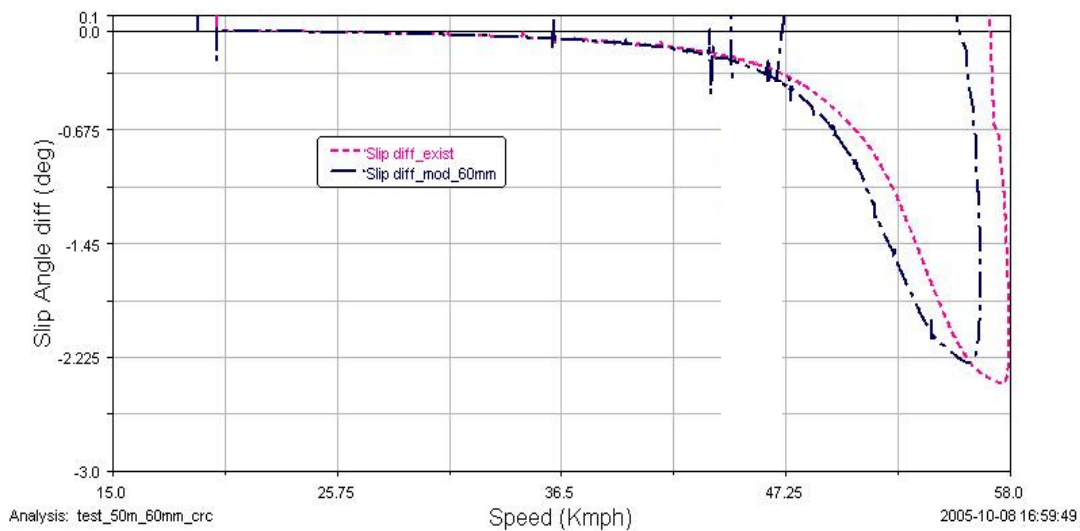


Figure 15: Variation of slip difference (front tire slip minus rear tire slip) with speed during cornering on 50 m radius: existing design, and modified design.

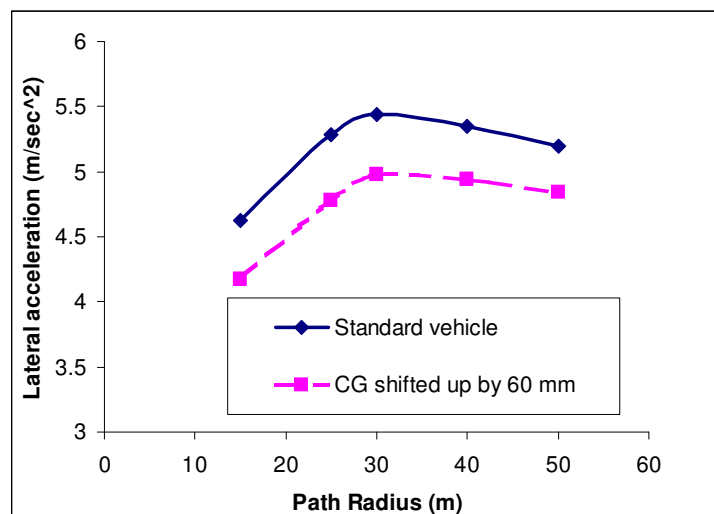


Figure 16: Variation of maximum lateral acceleration at which the roll over occurs with path radius. The interpolating curves are for visibility alone; the computed points are shown using markers that are found as described below. The vehicle is simulated on a circular path with low acceleration, and the forward speed keeps going up until the inner rear wheel leaves the

ground. Using the forward speed at that point, the lateral acceleration (v^2/R) is computed. The procedure is repeated for different radii.

Of the two curves shown in the figure, one corresponds approximately to the standard (existing) vehicle and the other to a chassis CG raised by 60 mm (correspondingly named in the figure labels). The two parameter sets are compared further in figure 16. It shows that the configuration with a higher CG will roll over at lower lateral accelerations compared to the standard model, which is expected. More interestingly, the lateral acceleration at impending tip-over depends significantly on the path radius. Analytical understanding of this effect could be taken up in future work.

4.2. Ramp climbing:

In this section, we present a simulation of the vehicle climbing a ramp as shown in figure 17.

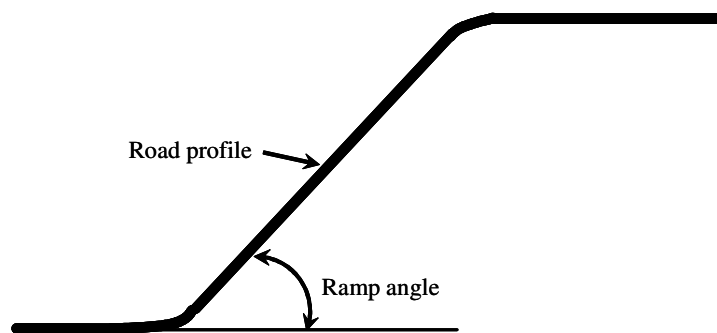


Figure 17: Schematic of a ramp to simulate vehicle-toppling.

The vehicle is simulated first on a straight flat path, then up a ramp of specified angle for about 25 m and finally again on a flat path (if it has not toppled backwards). The speed is kept at 6.95 m/sec and simulations are done with ramp angles ranging from 22 to 37 degrees.

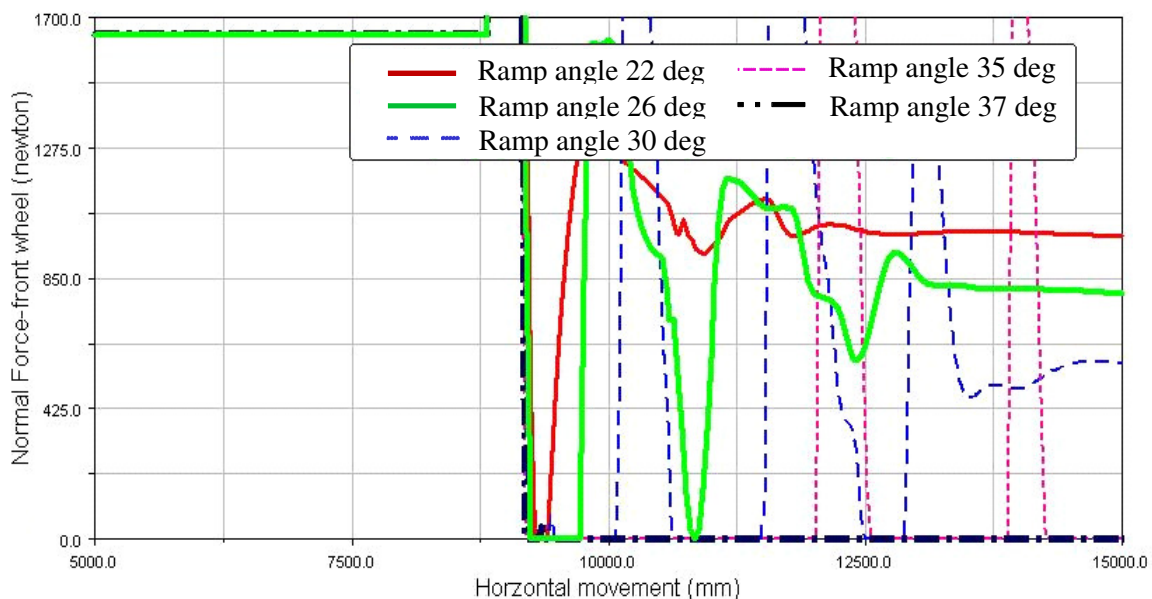


Figure 18: Variation of front wheel normal force with movement of vehicle on ramp.

The normal force at the front tire can be monitored to detect when the vehicle topples backwards. Results are shown in figure 18. Loss of contact at the front wheel occurs for all the ramp angles studied, and toppling occurs at ramp angles of about 35 degrees or more. A separate simple check using static moment balance about the rear axle (details not shown here) suggests toppling occurs under pseudo static conditions at ramp angles above 36.2 deg.

4.3. Linear eigenvalue analysis:

In this section we describe a simulation called linear eigenvalue analysis of the straight-running three-wheeler. This calculation is done using linearized quantities at an instant of interest, as will be clear below. In ADAMS-motorcycle the option for simulation of linear eigenvalue analysis (weave and wobble analysis) can be selected directly from the tab ‘Full vehicle analysis’ [5]. However in ADAMS-CAR a similar option is not available. Hence we have conducted this analysis using two steps as described below.

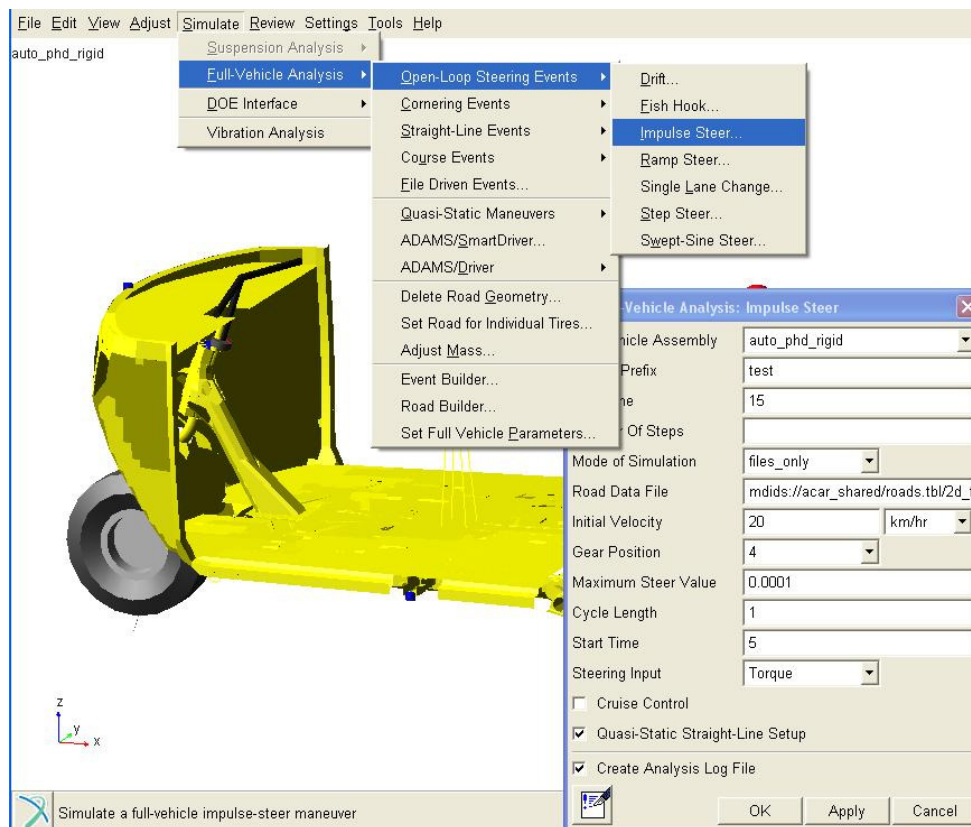


Figure 19: GUI of simulation type and input data prior to the linear eigenvalue analysis.

The aim of the first step is *only* to generate a final state that is to be used for linearized analysis in the second step. The final state of interest here is forward motion at a steady speed. Since the vehicle’s forward motion is known from prior simulation to be stable in this case, we have conducted a simulation of forward running with a small disturbance to the steering column. Figure 19 shows the selection of analysis and corresponding dialog box for this first step simulation. The sequence of selection of tabs is also shown in the same figure. We have chosen the “Impulse Steer” option. As suggested by entries in the box, a nominal speed of 20 km/hr. (5.56 m/sec) is specified. An impulse disturbance in the form of a steering torque is given at the fifth second in the simulation.

The steer value (maximum steer value in GUI) is kept very low to allow the vehicle to attain steady state within about a second. However, the simulations are performed up to 15 seconds to make sure transients are gone. The ‘files only’ option is chosen to save the output of the first step for subsequent use.

In the second step, ‘vibration analysis’ is selected from the tab ‘simulate’ of main menu. The dialog box is as shown in figure 20. In the box ‘simulation script name’ the name of the file saved from the first step is entered. ‘Normal mode analysis’ is chosen as shown in the figure (see [10] for further details) to find eigenvalues governing linearized dynamics of the vehicle at the 15th second (the final instant) of the first study.

Using the above two steps, the simulation is carried out for various speeds with two different choices of mechanical trail. Note that these simulations are performed for the rigid body model (no structural flexibilities).

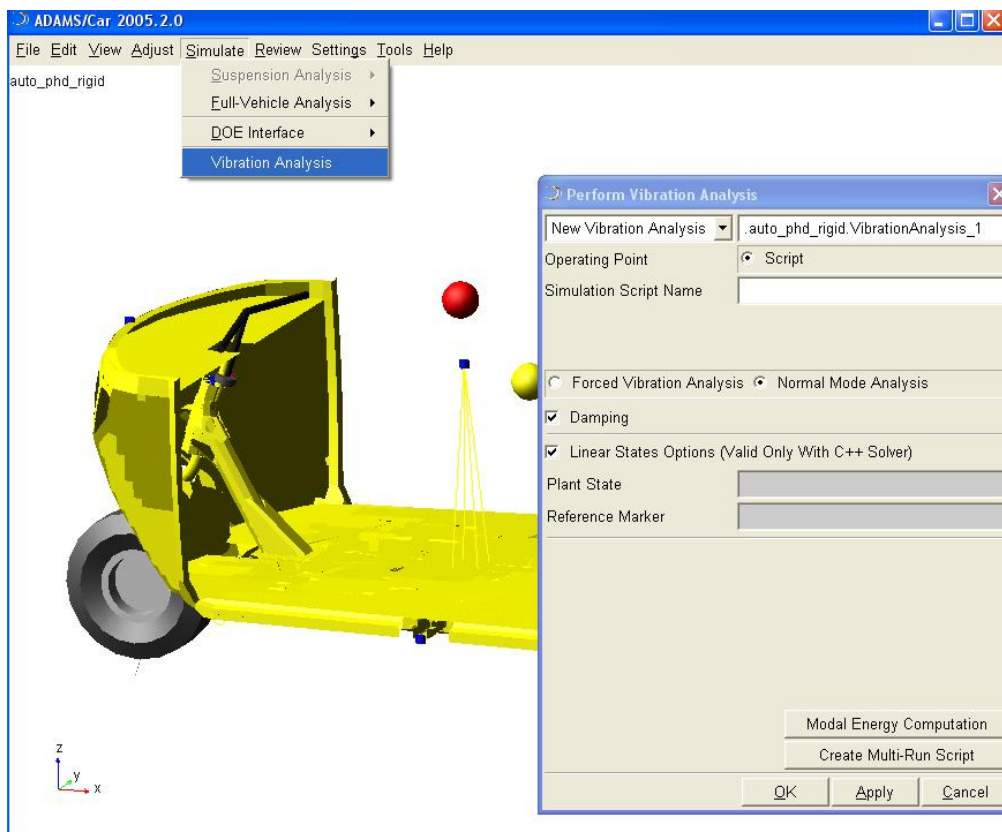


Figure 20: GUI of simulation tab for linear eigenvalue analysis

Eigenvalues obtained are discussed below. There are 50 eigenvalues including 6 rigid body modes (recall that the model has 25 degrees of freedom). Each mode shape was examined visually and only the steering oscillation mode is selected for presentation here. This mode predominantly involves steering oscillation, small body movements, and has low damping. The mode seems similar to the wobble mode of a two-wheeler, so we have called it a wobble mode. Figure 21a shows the imaginary parts of these wobble mode eigenvalues, each divided by 2π to give frequencies in Hz.

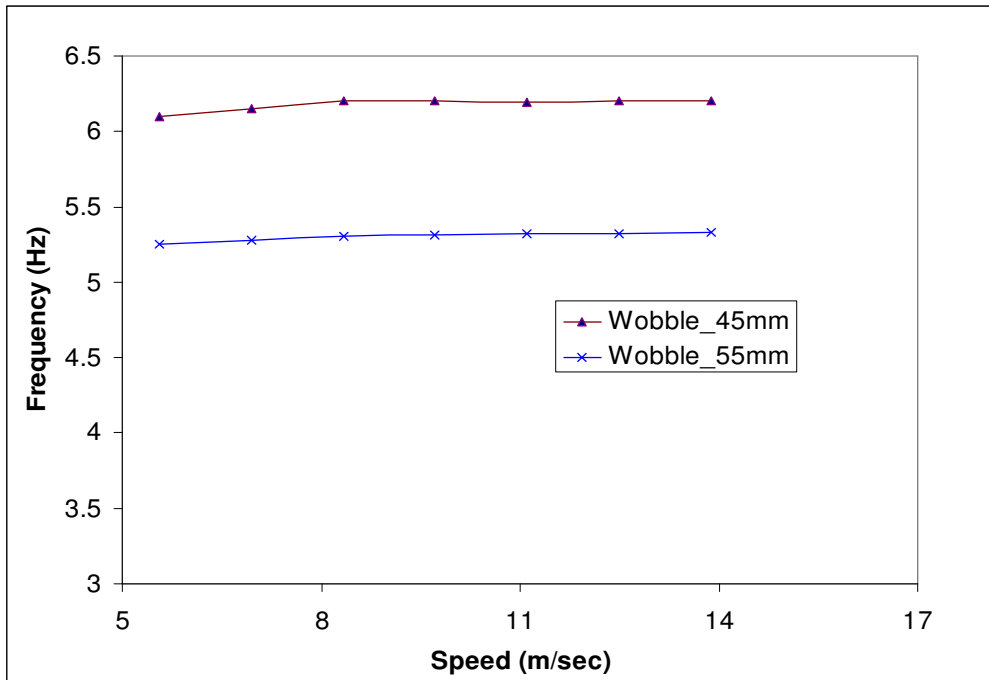


Figure 21a: Variation of wobble frequency with speed. The lines joining the points are for visibility alone.

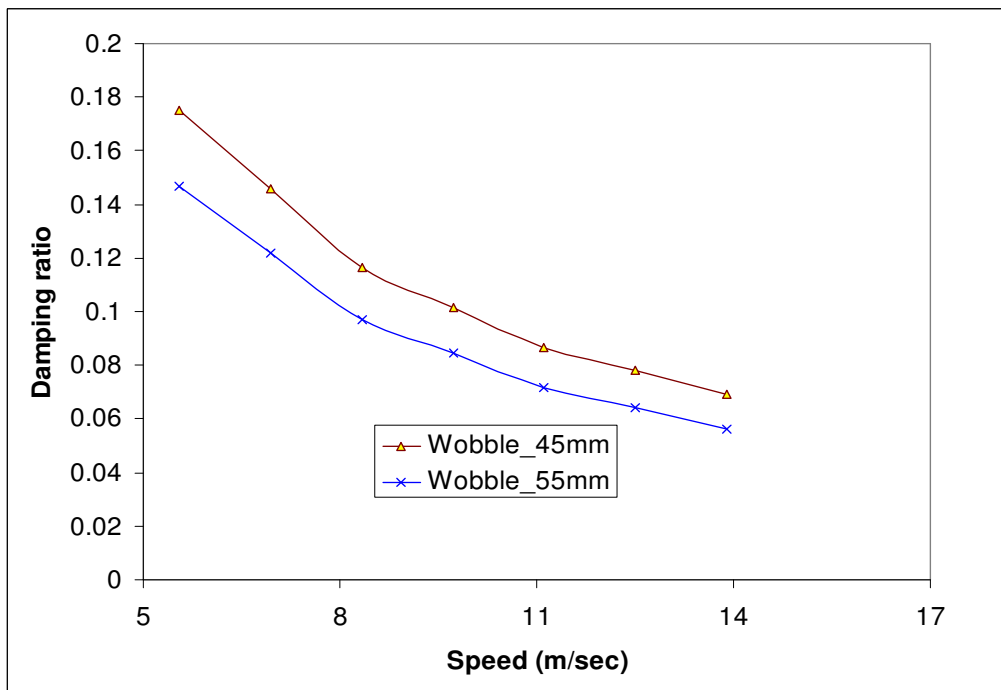


Figure 21b: Variation of wobble damping ratio with speed for rigid chassis. The lines joining the points are for visibility alone.

The frequency of oscillation is around 5.2 Hz for a 55 mm steering offset and around 6.1 Hz for a 45 mm steering offset. Further, figure 21b shows that the damping of the mode is positive at speeds up to 14 m/sec and even higher.

We end this section by mentioning an experimental observation. In the vehicle prototype, it has been observed that steering instability occurs in this vehicle at speeds below 8.33 m/sec. The frequency of that mode, measured experimentally, matches reasonably well with simulation. However, the simulation described above shows no unstable wobble mode in the rigid body model. The experimental observation has led us to study in further detail a dynamic model of the three-wheeler with flexibility included. The details of that investigation will be reported elsewhere.

5. Conclusions

A dynamic model for a three wheeled vehicle has been developed using ADAMS-CAR. The model could have up to 58 degrees of freedom, but detailed simulations have been conducted with a somewhat simplified model with 25 degrees of freedom. The procedure of developing the model is presented in some detail. The modelling of flexibility of major structural parts is also presented. Some simulations and results are presented. This study forms the basis of further ADAMS-based investigations of three wheeled vehicle dynamics, where new research questions can be addressed.

6. Acknowledgements

We thank the management of TVS Motor Co., Ltd., for permission to publish this work in the public domain.

7. References

1. V.M. Karanam and A. Chatterjee, "Common underlying steering curves for motorcycles in steady turns", *Vehicle system dynamics*, Vol. 49, No. 6, pp. 931-948, 2011.
2. R.S. Sharp, "Stability, control and steering responses of motorcycles", *Vehicle system dynamics*, Vol. 35, No. 4-5, pp. 291-318, 2001.
3. R.S. Sharp, S. Evangelou and D.J.N. Limebeer, "Advances in the modelling of motorcycle dynamics", *Multibody system dynamics*, No. 12, pp. 251-283, 2004.
4. V. Cossalter, R. Lot and F. Maggio, "The modal analysis of a motorcycle in straight running and on a curve", *Meccanica*, Vol. 39, pp. 1-16, 2004, Kluwer Academic Publishers, Printed in The Netherlands, ISSN 0025-6455.
5. V.M. Karanam and A. Chatterjee, "Some procedural details of analysis using ADAMS-Motorcycle". Available at <http://eprints.iisc.ernet.in/17639/>

6. Chul Kim and Paul I. Ro, "An accurate full car ride model using model reducing techniques", *Journal of mechanical design*, Vol. 124, Issue 4697, 2002.
7. N. Mirza, K. Hussain, A.J. Day and J. Klaps, "Investigation of the dynamic characteristics of suspension during braking", *Proceedings of the institution of mechanical engineers, Part D: Journal of Automobile engineering*, Vol. 219, No. 12, pp. 1429-1441, 2005.
8. V. Cossalter, N. Ruffo, F. Biral, R. Berritta and G. Cocco, "Development of a novel three wheeled vehicle", *Sicherheit umwelt zukunft III, Togungsband der, 3. Internationslen motorradkonferenz 2000*.
9. N. Amati, A. Festini, M. Porrati and A. Tonoli, "Coupling between lateral and vertical dynamics in three tilting wheels vehicles", Associazione Italiana per l'Analisi delle Sollecitazioni, 38th convegno nazionale, 2009-104. Available at <http://porto.polito.it/2308083/>
10. MSC.ADAMS/Car manual, MSC.Software, 2008.
11. MSC.ADAMS/Tire manual, MSC.Software, 2008.
12. H.B. Pacejka and E. Bakker, "The magic formula tyre model", *Vehicle system dynamics*, Vol. 21, Supplement 001, pp. 1-18, 1992.
13. H.B. Pacejka, "*Tire and vehicle dynamics*", Society of automotive engineers, 2006. <http://books.sae.org/book-r-372>

Appendix A

Shock-absorber bush properties

\$-----MDI_HEADER

[MDI_HEADER]

FILE_TYPE = 'bus'

FILE_VERSION = 4.0

FILE_FORMAT = 'ASCII'

\$-----UNITS

[UNITS]

LENGTH = 'mm'

ANGLE = 'degrees'

FORCE = 'newton'

MASS = 'kg'

TIME = 'second'

\$-----DAMPING

[DAMPING]

FX_DAMPING = 28.0

FY_DAMPING = 28.0

FZ_DAMPING = 3.5

TX_DAMPING = 0.62

TY_DAMPING = 0.62

TZ_DAMPING = 0.12

\$-----FX_CURVE

[FX_CURVE]

{ x fx }

-3.0 -20000.0

-2.4 -6000.0

-1.8 -2500.0

-1.2 -950.0

-0.6 -330.0

0.0 0.0

0.6 330.0

1.2 950.0

1.8 2500.0

2.4 6000.0

3.0 20000.0

\$-----FY_CURVE

[FY_CURVE]

{ y fy }

-3.0 -20000.0

-2.4 -6000.0

-1.8 -2500.0

-1.2 -950.0

-0.6 -330.0

0.0 0.0

0.6 330.0

1.2 950.0

1.8 2500.0

2.4 6000.0

3.0 20000.0

\$-----FZ_CURVE

```
[FZ_CURVE]
{ z    fz}
-3.0 -20000.0
-2.4 -6027.9617
-1.8 -2000.0
-1.2 -400.0
-0.6 -42.0
0.0 0.0
0.6 42.0
1.2 400.0
1.8 2000.0
2.4 6000.0
3.0 20000.0
```

\$-----TX_CURVE

```
[TX_CURVE]
{ ax    tx}
-10.0 -620.0
-8.0 -496.0
-6.0 -372.0
-4.0 -248.0
-2.0 -124.0
0.0 0.0
2.0 124.0
4.0 248.0
6.0 372.0
8.0 496.0
10.0 620.0
```

\$-----TY_CURVE

```
[TY_CURVE]
{ ay    ty}
-10.0 -620.0
-8.0 -496.0
-6.0 -372.0
-4.0 -248.0
-2.0 -124.0
0.0 0.0
2.0 124.0
4.0 248.0
6.0 372.0
8.0 496.0
10.0 620.0
```

\$-----TZ_CURVE

```
[TZ_CURVE]
{ az    tz}
-10.0 -120.0
-8.0 -96.0
-6.0 -72.0
-4.0 -48.0
-2.0 -24.0
0.0 0.0
2.0 24.0
4.0 48.0
6.0 72.0
```

8.0 96.0
10.0 120.0

Appendix B

Rear trailing arm bush properties

\$-----MDI_HEADER

[MDI_HEADER]
FILE_TYPE = 'bus'
FILE_VERSION = 4.0
FILE_FORMAT = 'ASCII'

\$-----UNITS

[UNITS]
LENGTH = 'mm'
ANGLE = 'degrees'
FORCE = 'newton'
MASS = 'kg'
TIME = 'second'

\$-----DAMPING

[DAMPING]
FX_DAMPING = 98.0
FY_DAMPING = 98.0
FZ_DAMPING = 8.5
TX_DAMPING = 3.0
TY_DAMPING = 3.0
TZ_DAMPING = 0.24

\$-----FX_CURVE

[FX_CURVE]
{ x fx}
-4.0 -20000.0
-3.2 -8000.0
-2.4 -4000.0
-1.6 -2000.0
-0.8 -784.0
0.0 0.0
0.8 784.0
1.6 2000.0
2.4 4000.0
3.2 8000.0
4.0 20000.0

\$-----FY_CURVE

[FY_CURVE]
{ y fy}
-4.0 -20000.0
-3.2 -8000.0
-2.4 -4000.0
-1.6 -2000.0
-0.8 -784.0
0.0 0.0
0.8 784.0
1.6 2000.0
2.4 4000.0
3.2 8000.0

```

4.0 20000.0
$-----FZ_CURVE
[FZ_CURVE]
{ z    fz}
-4.0 -1000.0
-3.2 -500.0
-2.4 -250.0
-1.6 -136.0
-0.8 -68.0
0.0 0.0
0.8 68.0
1.6 136.0
2.4 204.0
3.2 500.0
4.0 1000.0
$-----TX_CURVE
[TX_CURVE]
{ ax    tx}
-5.0 -1480.0
-4.0 -1184.0
-3.0 -888.0
-2.0 -592.0
-1.0 -296.0
0.0 0.0
1.0 296.0
2.0 592.0
3.0 888.0
4.0 1184.0
5.0 1480.0
$-----TY_CURVE
[TY_CURVE]
{ ay    ty}
-5.0 -1480.0
-4.0 -1184.0
-3.0 -888.0
-2.0 -592.0
-1.0 -296.0
0.0 0.0
1.0 296.0
2.0 592.0
3.0 888.0
4.0 1184.0
5.0 1480.0
$-----TZ_CURVE
[TZ_CURVE]
{ az    tz}
-10.0 -240.0
-8.0 -192.0
-6.0 -144.0
-4.0 -96.0
-2.0 -48.0
0.0 0.0
2.0 48.0
4.0 96.0

```

6.0 144.0
 8.0 192.0
 10.0 240.0

Appendix C

Tire properties

```

! :FILE_TYPE:   tir
! :FILE_VERSION: 2
! :TIRE_VERSION: PAC94
! :COMMENT:     New File Format v2.1
! :FILE_FORMAT: ASCII
! :TIMESTAMP:   1996/02/15,13:22:12
! :USER:        ncos
$-----units
[UNITS]
LENGTH      = 'mm'
FORCE       = 'newton'
ANGLE       = 'radians'
MASS        = 'kg'
TIME        = 'second'
$-----model
[MODEL]
! use mode          1      2      3      4
!
! smoothing                X      X
! combined                X      X
!
! USER_SUB_ID = 903
PROPERTY_FILE_FORMAT = 'PAC94'
FUNCTION_NAME      = 'TYR903'
USE_MODE          = 4
$-----dimensions
[DIMENSION]
UNLOADED_RADIUS    = 203.0
WIDTH              = 101.0
ASPECT_RATIO       = 1.00
$-----parameter
[PARAMETER]
VERTICAL_STIFFNESS = 160.0
VERTICAL_DAMPING   = 0.0557
LATERAL_STIFFNESS  = 160.0
$-----scaling
[SCALING_COEFFICIENTS]
DLAT = 0.10000E+01
DLON = 0.10000E+01
BCDLAT = 0.10000E+01
BCDLON = 0.10000E+01
$-----lateral
[LATERAL_COEFFICIENTS]
A0 = 0.5
A1 = -1300
A2 = 2400

```

A3 = -250
A4 = -3
A5 = -0.0024
A6 = -1.6
A7 = 1.6
A8 = 0.0
A9 = 0.0
A10 = 0.0
A11 = 0.0
A12 = -130
A13 = 0.0
A14 = 0.0
A15 = -0.1
A16 = 0.0
A17 = 0.2

\$-----longitudinal

[LONGITUDINAL_COEFFICIENTS]

B0 = 1.49
B1 = -30
B2 = 900
B3 = 101.34
B4 = -172.6
B5 = -0.06176
B6 = 0.015667
B7 = 0.1855
B8 = 1.0
B9 = 0
B10 = 0
B11 = 0.000000E+00
B12 = 0.000000E+00
B13 = 0.000000E+00

\$-----aligning

[ALIGNING_COEFFICIENTS]

C0 = 3.9
C1 = 0
C2 = -7.8
C3 = -0.05
C4 = -2
C5 = 0.15
C6 = 0
C7 = -0.01
C8 = -0.2
C9 = -0.62
C10 = 0.036
C11 = 0
C12 = 0
C13 = -0.0177
C14 = 1
C15 = 0
C16 = 0.413
C17 = -0.2357
C18 = 6.0754417E-03
C19 = -4.2525059E-01
C20 = -2.1503067E-01

\$-----shape

[SHAPE]

{radial width}

1.0 0.0
1.0 0.2
1.0 0.4
1.0 0.5
1.0 0.6
1.0 0.7
1.0 0.8
1.0 0.85
1.0 0.9
0.9 1.0